TESTING THE DELTAIC ORIGIN OF FAN DEPOSITS AT BRADBURY CRATER, MARS.
M. S. Bramble[1], T. A. Goudge[2], R. E. Milliken[1], and J. F. Mustard[1], [1]Dept. of Earth, Environmental, and Planetary Sciences, Brown University, Providence, RI, 02912 (Michael_Bramble@brown.edu), [2]Jackson School of Geosciences, The University of Texas at Austin, Austin, TX.

Introduction: Bradbury crater is a 60 km diameter impact crater in Libya Montes. This region is the remnant cratered southern rim of the Isidis basin where dissected massifs and craters are superposed by volcanic plains and carved by valleys [1–3]. The greater region has experienced multiple extensive episodes of aqueous activity as evidenced by the valley networks carved through the Montes that flow towards Isidis Planitia [1], and by the various hydrous minerals identified in multiple geologic units [2].

Previous studies of Bradbury crater identified landforms that were interpreted as fluvial and lacustrine deposits resulting from the past presence of lakes, seas, and oceans [3]. *Erkeling et al.* [3] and more recent work [4–7] interpreted specific depositional environments for identified sedimentary deposits in Bradbury crater. Three deposits have been discussed in particular, and they are found isolated to the north, east, and west (N, E, and W) of the crater center (**Figure 1**). The E deposit was suggested to have been formed in a body of standing water, as it is found in a 3 km diameter depression termed an open paleolake by [3,5] as both inlet and outlet channels are observed to the immediate north and south (**Figure 1b**). The W deposit was identified as an alluvial fan formed from Noachian fluvial activity [3]. The N deposit sits in the northernmost of two possibly highly eroded impact craters that formed on the crater rim producing the breach towards Isidis Planitia [7]. Subsequent mapping of these deposits using High Resolution Imaging Science Experiment (HiRISE) images was used to suggest the presence of topsets, foresets, and bottomsets indicative of a deltaic system based on the morphology of the fan shapes [4,5], and the N deposit has been identified as a delta by several contributions [3–7]. However, the stratal geometry of these landforms and lateral and vertical changes in bedding dip angles and orientations have not been quantitatively assessed. In this study we investigate these deposits using HiRISE data and apply quantitative stratigraphic methods, where possible, to test the purported deltaic origin of these deposits.

The term delta is a hard-won geological expression referring to a protuberance of sediment formed when a river enters a standing body of water, reducing the current velocity, and forming a generally coarsening upwards sequence. Additionally, and as first described in the 19th Century by G. K. Gilbert, deltas exhibit a facies of flat-lying topsets, steeply dipping foresets, and flat-lying bottomsets [8]. The progression of layer angles in a deltaic system provides a stratigraphic signature that can be investigated using high-resolution remote sensing data, as has been shown by several geometric analyses of martian fan-shaped deposit stratigraphy [9–12].

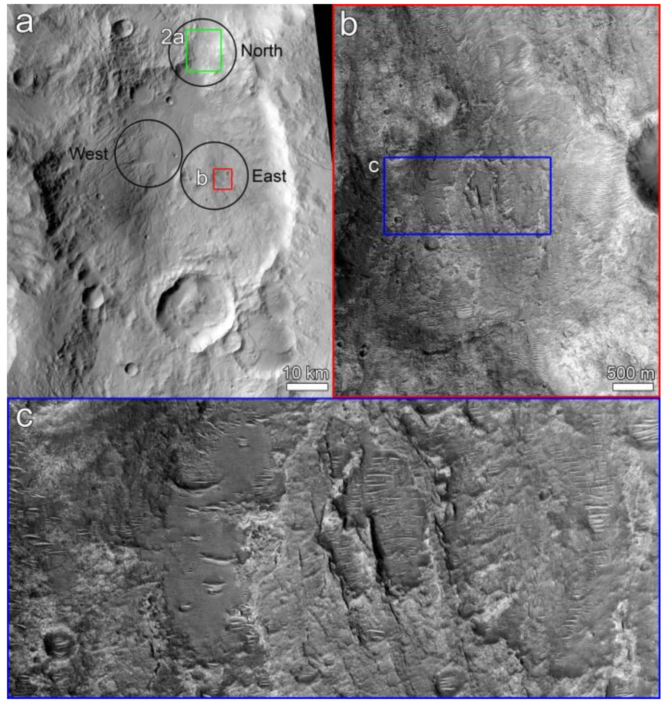

Figure 1: (a) CTX Mosaic of Bradbury crater. Three circles identify the deposits analyzed in this study. (b) Subframe of HiRISE image ESP_038530_1830 depicting the eastern deposit. (c) Subframe of (b) detailing the meter-scale morphology of the E deposit. No meter-scale layering is observed. A decameter-scale stratigraphy is observed of light-toned material overlain by a dark-toned crater-preserving surface. Possible inverted channels are observed at the uppermost surface. North is up in each frame.

Methods: We apply modified methods of [12] to investigate the stratigraphic architecture of the fan deposits at Bradbury crater. All three deposits were qualitatively analyzed using orthorectified HiRISE images and digital elevation models (DEMs) produced using HiRISE stereo pairs and the NASA Ames Stereo Pipeline [13–15].

For quantitative analysis of the N deposit and to minimize errors from regional topography, the High Resolution Stereo Camera (HRSC) [16,17] DEM h2162_0002 was tied to MOLA [18] point shot data, and then the HiRISE DEM was tied to the corrected HRSC DEM [19]. Discernable layers in the N deposit

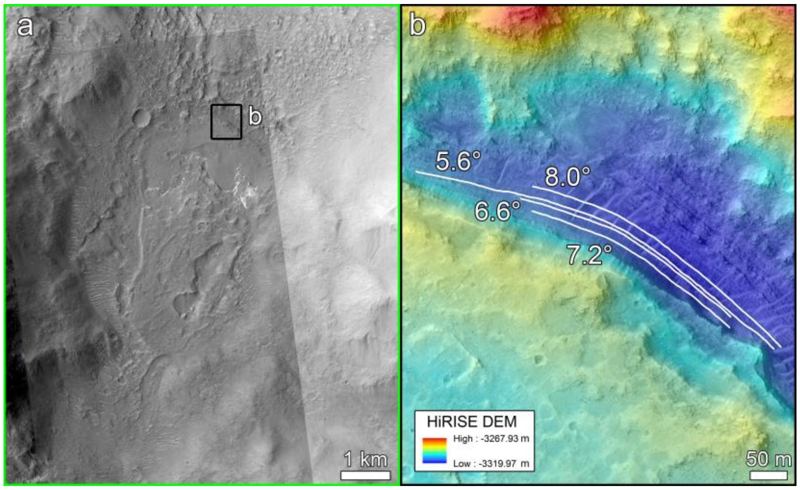

Figure 2: The north deposit of Bradbury crater. (a) Subframe of HiRISE image PSP_007727_1830 depicting the north deposit. The lobate shape of the deposit is visible, as well as the large-scale stratigraphy observed at the other two deposits. (b) HiRISE DEM made from the image in (a) and PSP_008808_1830. Colorized elevation of the deposit depicting the topography of the layered sequence. The white lines show fit layers and calculated dip angles are shown. North is up in each frame.

that were >50 m in length were mapped and location information of these layers was sampled at 2 m intervals in three dimensions. Following the methods of [12] and the references therein, planes were fit to the extracted layer position data using a linear least squares method [e.g., 9–11]. Fits were recorded if the variance explained by the first principal component in a principal component analysis was <99.5% and the ratio of the variance explained by the second and third principal component was >15 [20].

Results: Though crudely stratified, the E and W deposits do not exhibit layering of sufficient resolution and continuity for quantitative analysis. Both deposits have similar decameter-scale stratigraphy that includes a meters-thick, light-toned, mottled unit containing dark-toned fractures overlain by a dark-toned unit with a rough, corrugated surface texture (**Figure 1c**).

The N deposit, which resides in a topographic depression, is strikingly different and displays a fan shape with layering (**Figure 2a**). Robust fits from four layers evenly spaced throughout the sequence (**Figure 2b**) show an approximately constant dip of 7.1 ± 0.6° and strike of 307.6 ± 4.3°, steeper than the ~2° regional slope through the breach in the crater wall. Ongoing work will focus on increasing the number of measured layers to improve statistics.

Discussion and Implications: Morphologic and stratigraphic analysis of Bradbury crater's three fan-shaped deposits reveals no clear evidence for continuous bedding at the meter scale in the E and W deposits, and approximately constant layer dips throughout the layered section in the N deposit.

The constant dip observed throughout the layered section in the N deposit may be indicative of deposition in an alluvial, debris, or volcanic flow environment. The high layer dip angles could only be consistent with deltaic foresets and not topsets or bottomsets; however, the layered sequence is observed at the terminus of the N deposit in a region mapped as bottomsets by [3–5]. Instead, the ~7° slope is consistent with an alluvial/debris-flow fan origin. Importantly, we find no clear evidence for changes in bedding geometry that would imply emplacement in standing water or transitions in water depth. Quantitative stratigraphic analysis of the N deposit at Bradbury crater conclusively shows this deposit is not consistent with a deltaic origin. The E and W deposits lack observable layered sequences, but from morphologic investigation no systematic evidence suggesting that they were formed in a deltaic environment has been observed. Therefore, there is no conclusive evidence for a sustained standing body of water having been present in Bradbury crater, nor the small circular depressions in the rim-breaching valley, during formation of the fan deposits.

Alluvial and fluvial processes may be responsible for these features, possibly related to the fluvial activity that carved channels here and in the wider Libya Montes region. The amount of water that may have been present in Bradbury is thus more poorly constrained compared with deposits elsewhere on Mars that exhibit orbital-scale stratigraphic architecture consistent with a deltaic environment.

References: [1] Jaumann R. et al. (2010) *EPSL*, 294, 272–290. [2] Bishop J. L. et al. (2013) *JGR*, 118, 487–513. [3] Erkeling G. et al. (2012) *Icarus*, 219, 393–413. [4] Erkeling G. et al. (2015) *LPS XLVI*, Abstract #1779. [5] Erkeling G. et al. (2016) *LPS XLVII*, Abstract #1451. [6] Tirsch D. et al. (2015) *LPS XLVI*, Abstract #1738. [7] Tirsch D. et al. (2016) *LPS XLVII*, Abstract #1444. [8] Allaby M. (2008) *Oxford University Press*, NY, NY. 654 pp. [9] Lewis K. W. and Aharonson O. (2006) *JGR*, 111, E06001. [10] Ansan V. et al. (2011) *Icarus*, 211, 273–304. [11] DiBiase R. A. et al. (2013) *JGR*, 118, 1285–1302. [12] Goudge T. A. et al. (2017) *EPSL*, 458, 357–365. [13] Broxton M. J. and Edwards L. J. (2008) *LPS XXXIX*, Abstract #2419. [14] Moratto Z. M. et al. (2010) *LPS XLI*, Abstract #2364. [15] Shean, D. E. et al. (2016) *ISPRS J. Photogramm. Remote Sens.*, 116, 101–117. [16] Neukum G. et al. (2004) *Eur. Space Agency Spec. Publ.*, 1240, 17–35. [17] Gwinner K. F. et al. (2010) *EPSL*, 294, 506–519. [18] Smith D. E. et al. (2001) *JGR*, 106, 23689–23722. [19] Beyer R. A. et al. (2014) *LPS XLV*, Abstract #2902. [20] Lewis K. W. et al. (2008) *JGR*, 113, E12S36.